Mechanical Properties of Formamidinium Halide Perovskites $FABX_3$ (FA=$CH(NH_2)_2$; B=Pb, Sn; X=Br, I) by First-Principles Calculations *

Lei Guo(郭磊), Gang Tang(唐刚), Jiawang Hong(洪家旺)**

School of Aerospace Engineering, Beijing Institute of Technology, Beijing 100081

(Received 1 March 2019)

The mechanical properties of formamidinium halide perovskites $FABX_3$ (FA=$CH(NH_2)_2$; B=Pb, Sn; X=Br, I) are systematically investigated using first-principles calculations. Our results reveal that $FABX_3$ perovskites possess excellent mechanical flexibility, ductility and strong anisotropy. We shows that the planar organic cation FA^+ has an important effect on the mechanical properties of $FABX_3$ perovskites. In addition, our results indicate that (i) the moduli (bulk modulus B, Young's modulus E, and shear modulus G) of $FABBr_3$ are larger than those of $FABI_3$ for the same B atom, and (ii) the moduli of $FAPbX_3$ are larger than those of $FASnX_3$ for the same halide atom. The reason for the two trends is demonstrated by carefully analyzing the bond strength between B and X atoms based on the projected crystal orbital Hamilton population method.

PACS: 62.20.−x, 63.20.dk, 71.15.Mb, 71.20.Nr DOI: 10.1088/0256-307X/36/5/056201

In recent years, the power conversion efficiency of organic–inorganic hybrid perovskites (OIHPs) ABX_3 (A=MA (CH_3NH_3); FA ($CH(NH_2)_2$); B=Pb, Sn; X=I, Br) has increased from 3.81% to 23.7%,[1–5] which has attracted great attention to investigations of superior photovoltaic performances and various potential optoelectronic applications. Experimental and theoretical investigations have confirmed that the excellent optoelectronic properties of OIHPs result from several advantages, such as the suitable direct band gap, defect tolerance, long carrier lifetime and diffusion length.[6–8] In addition to the advantages mentioned above, another advantage of OIHPs compared to their inorganic counterparts is the soft nature of the hybrid framework, providing possible applications in flexible and wearable electronic devices. Recently, it was reported that stress and strain existing in hybrid perovskites play a critical role in film stability and device performance.[9,10] Consequently, research on the mechanical properties and deformation behavior of OIHPs has attracted widespread attention.

Feng[11] and Roknuzzaman *et al.*[12] theoretically investigated the mechanical properties of methylammonium halide perovskite $MABX_3$ (B=Sn, Pb; X=Br, I) using the first-principles method. Subsequently, some experimental techniques such as nanoindentation, sound velocity measurement and inelastic neutron scattering were also employed to investigate the elastic properties of OIHP $MABX_3$ (B=Pb; X=I, Br) at room temperature.[13–15] Compared to $MABX_3$, formamidinium halide perovskite $FABX_3$ (FA=$CH(NH_2)_2$, B=Pb, Sn, X=I, Br) has a more optimal electronic band gap, superior thermal stability and a lower hysteresis.[16–18] However, the mechanical properties of $FABX_3$ need further investigation to understand its flexible nature.

In this work, the mechanical properties and bonding characteristics of $FABX_3$ (B=Sn, Pb; X=Br, I) compounds were systematically investigated using first-principles calculations. Our results show that $FABX_3$ perovskites are mechanically flexible and ductile. It is also observed that $FABX_3$ perovskites exhibit strong anisotropy on the mechanical properties. We find that the organic cation FA^+ structure plays an important role in the shear elastic constants. Finally, two general tendencies are obtained as follows: (i) Replacing I with Br, the values of the moduli (bulk modulus B, Young's modulus E and shear modulus G) increase in Pb-based and Sn-based perovskites. (ii) Replacing Pb with Sn, the values of the moduli decrease in I-based and Br-based perovskites. The reasons were revealed by carefully analyzing the B–X bonding characteristics in $FABX_3$ based on the projected crystal orbital Hamilton population (pCOHP) method.

Our calculations are performed using the Vienna *ab initio* simulation package (VASP) code in the framework of density function theory.[19,20] The electron–ion interaction is described by the projector augmented wave method.[21] The plane-wave cut-off energy was set to 840 eV. The $9 \times 9 \times 9$ Monkhorst–Pack k-point mesh was employed for sampling the Brillouin zone. Both the k-point mesh and the cut-off energy were tested carefully for the convergence. The lattice parameters and atomic positions were fully relaxed until the energy difference was less than 10^{-4} eV and the force on each atom was smaller than 10^{-2} eV/Å. In this work, the PBE+vdW-DF2 method was used to consider the van der Waals interactions, which plays an important role in the hybrid perovskite materials with weak interactions along the stacking direction.[22,23] We utilized the package Lob-

*Supported by the National Natural Science Foundation of China under Grant No 11572040, the Thousand Young Talents Program of China, and the Special Program for Applied Research on Super Computation of the NSFC-Guangdong Joint Fund (second phase) under Grant No U1501501.

**Corresponding author. Email: hongjw@bit.edu.cn

© 2019 Chinese Physical Society and IOP Publishing Ltd

ster to compute the crystal orbital Hamiltonian population (COHP) for the bonding analysis.[24,25] Mechanical properties are calculated by the finite difference method in VASP.[26]

According to previous experiments, $FABX_3$ mainly adopts a cubic crystal structure at room temperature.[27] Our calculations are based on the $FAPbI_3$ cubic structure obtained from the experiment (space group: $Pm3m$, lattice constant: 6.36 Å, atomic position: Pb (0.0, 0.0, 0.0), I (0.5, 0.0, 0.0), C (0.5, 0.57, 0.5), N (0.68, 0.48, 0.5), H (0.5, 0.74, 0.5), H (0.81, 0.57, 0.5), H (0.70, 0.32, 0.5)).[27] The crystal structure of $FABX_3$ is shown in Fig. 1. The center of the octahedron is occupied by the B atom, the X atoms share the corner positions of the octahedron, and the organic cation FA lies in a cage surrounded by $[PbX_6]$ octahedrons. Following the previous theoretical work,[28,29] we fully relax the atomic coordinates and lattice parameters from the experimental cubic structure and obtain the pseudo-cubic structure. As can be seen in Table 1 (X_a, X_b, X_c represents the halide X atom along the a, b, c axes, respectively), the calculated lattice constants are slightly larger than the experimental data[27,30–32] owing to the overestimation of the PBE method. We can also see that replacing I (Pb) with smaller Br (Sn) atoms, the lattice constant of $FABX_3$ decreases, showing the same trend as the experimental values. Due to the influence of organic cation FA^+, the B–$X_{a(c)}$–B angles are not equal to 180°, illustrating that $X_{a(c)}$ is away from the a (c) axis direction, leading to slight distortion of the $FABX_3$ structure.

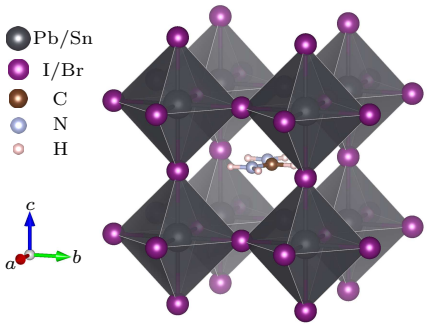

Fig. 1. The cubic structure of $FABX_3$.

Table 1. Lattice parameters and atomic bonds of $FABX_3$ perovskites.

$FABX_3$			$FAPbI_3$	$FAPbBr_3$	$FASnI_3$	$FASnBr_3$
Lattice constant (Å)	This work	a	6.67	6.30	6.62	6.26
		b	6.50	6.08	6.46	6.03
		c	6.61	6.21	6.53	6.14
	Expt.[27,30–32]	$a/b/c$	6.36	5.99	6.32	6.03
Bond angle (deg)		B–X_a–B	178.9	178.0	176.7	179.0
		B–X_b–B	180.0	180.0	180.0	180.0
		B–X_c–B	174.4	175.0	171.5	172.5
Bond length (Å)		B–X_a	3.34	3.15	3.31	3.13
		B–X_b	3.22	3.03	3.04	2.83
		B–X_c	3.31	3.11	3.28	3.08

Table 2. Elastic constants of $FABX_3$ perovskite compounds from calculations and experiment in units of GPa.

$FABX_3$	C_{11}	C_{22}	C_{33}	C_{44}	C_{55}	C_{66}	C_{12}	C_{13}	C_{23}
$FAPbI_3$	30.15	31.00	29.85	2.03	5.33	2.60	2.99	7.22	4.26
Calc.[33]	20.50			4.80			12.30		
$FAPbBr_3$	37.98	45.21	34.59	3.34	5.30	1.85	7.26	9.95	5.65
Expt.[13]	31.2±0.2			1.5±0.1			4± 0.5		
Expt.[13]	27.7±1.6			3.1±0.1			11.5±2.4		
$FASnI_3$	29.96	25.21	26.02	2.35	4.90	2.41	6.85	8.23	3.28
$FASnBr_3$	35.34	26.66	32.13	3.29	5.65	1.21	5.72	10.85	3.77

The elastic constants of $FABX_3$ perovskites are obtained from first-principles calculations, as listed in Table 2. Our calculated elastic constants of these hybrid halide perovskites satisfy the elastic stability conditions, suggesting that all structures are mechanically stable.[34–36] The calculated C_{11}, C_{44} and C_{12} by this work are slightly larger than the experimental results[13] and the data calculated by Wang *et al.*,[33] and the elastic constants C_{11}, C_{22} and C_{33} are larger than the other elastic constants, implying strong resistance to stretch along the [100] ([010] or [001]) direction but weak resistance to shear deformation for $FABX_3$ compounds. This is consistent with the observation from recent experimental works.[13] Interestingly, we note that C_{55} is relatively larger than C_{44} and C_{66} for all the compounds, which implies a better ability to resist shear deformation in the (010) crystal plane than the (100) and (001) planes. Here C_{13} is also relatively larger compared to C_{12} and C_{23}. The fact that C_{55} is larger than C_{44} and C_{66} indicates stronger couplings between directions a and c than those between directions a and b or b and c, which also induces the C_{13} larger than C_{12} and C_{23}. This may result from the halide X, which distorts away from the a and c axes in such a pseudo-cubic structure due to the orientation of the planar organic cation FA^+.

The elastic moduli are calculated by[36]

$$B_{\rm V} = \frac{1}{9}(C_{11}+C_{22}+C_{33}) + \frac{2}{9}(C_{12}+C_{13}+C_{23}), \quad (1)$$

$$G_{\rm V} = \frac{1}{15}(C_{11}+C_{22}+C_{33}) - \frac{1}{15}(C_{12}+C_{13}+C_{23}) + \frac{1}{5}(C_{44}+C_{55}+C_{66}), \quad (2)$$

$$B_{\rm R} = \frac{1}{(S_{11}+S_{22}+S_{33})+2(S_{12}+S_{13}+S_{23})}, \quad (3)$$

$$G_{\rm R} = 15/[4(S_{11}+S_{22}+S_{33}) - 4(S_{12}+S_{13}+S_{23}) + 3(S_{44}+S_{55}+S_{66})], \quad (4)$$

where S_{ij} is the elastic compliance matrix. The bulk modulus B, shear modulus G, Young's modulus E, Poisson's ratio ν, Pugh's ratio B/G,[37] and universal anisotropy index $A^{\rm U}$[38] of these perovskite compounds were calculated using the Voigt–Reuss–Hill approximation, and the relationships are given as

$$B = \frac{B_{\rm V}+B_{\rm R}}{2}, \quad (5)$$

$$G = \frac{G_{\rm V}+G_{\rm R}}{2}, \quad (6)$$

$$E = \frac{9BG}{(3B+G)}, \quad (7)$$

$$v = \frac{3B-2G}{[2(3B+G)]}, \quad (8)$$

$$A^{\rm U} = 5\frac{G_{\rm V}}{G_{\rm R}} + \frac{B_{\rm V}}{B_{\rm R}} - 6. \quad (9)$$

As listed in Table 3, the calculated bulk modulus of $FAPbBr_3$ (18.34 GPa) is in good agreement with the experimental data (16.9 ± 1.7 GPa).[13] In terms of Young's modulus E, our results are relatively larger than the experimental values.[15] The ductility of a material has been extensively indexed by the critical value 1.75 for Pugh's ratio (0.26 for Poisson's ratios). In other words, the material will be ductile (brittle) if Pugh's ratio or Poisson's ratios is larger (smaller) than 1.75 or 0.26.[11,37] Our results show that all the calculated perovskites have large B/G (from 2.37 to 2.88) and ν (from 0.31 to 0.34), which indicates that $FABX_3$ exhibits a good ductility suitable for flexible materials. Moreover, Pugh's ratio of the Br-based perovskites in this study ($FAPbBr_3$ and $FASnBr_3$) is the largest (larger than 2.8), suggesting that they are the most ductile materials in these compounds. In addition, we notice that the Br-based perovskites exhibit stronger anisotropic properties compared with I-based perovskites according to the universal anisotropy index $A^{\rm U}$, as well as the three-dimensional (3D) surface contours of Young's modulus (Fig. 2). This strong anisotropy indicates that Br-based perovskites will be more unstable than I-based perovskites under ambient conditions.[11,39] Compared with MA-based organic–inorganic perovskites,[11] all of them possess excellent mechanical flexibility and ductility, and strong anisotropy. In addition, Young's moduli of FA-based perovskites are lower than that of MA-based perovskites, which are due to the larger FA^+ weakening the inorganic framework.[15]

Table 3. Calculated and experimental mechanical parameters of $FABX_3$, including Bulk modulus B, shear modulus G, Young's modulus E, Poisson's ratio ν, Pugh's ratio B/G and universal anisotropy index $A^{\rm U}$. For the mechanical moduli, the unit is GPa.

$FABX_3$	B	G	E	B/G	ν	$A^{\rm U}$
$FAPbI_3$	13.25	5.59	14.70	2.37	0.31	3.68
Calc.[33]	15.30	3.60	9.90	4.30	0.4	
Expt.			(11.8.±1.9)[15]			
$FAPbBr_3$	18.34	6.37	17.11	2.88	0.34	4.75
Expt.	(16.9.±1.7)[13]		(12.3.±0.8)[15]			
$FASnI_3$	12.96	5.08	13.48	2.55	0.33	2.60
$FASnBr_3$	14.64	5.18	13.88	2.83	0.34	5.27

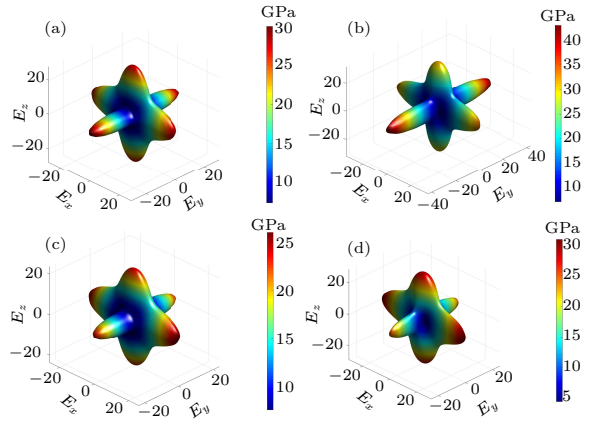

Fig. 2. 3D surface contour of Young's modulus for (a) $FAPbI_3$, (b) $FAPbBr_3$, (c) $FASnI_3$, and (d) $FASnBr_3$.

We also observe two general tendencies: (i) Replacing I with Br, the values of bulk modulus, shear modulus and Young's modulus increase in Pb/Sn-based perovskites. (ii) Replacing the Pb with Sn, the values of bulk modulus, shear modulus and Young's modulus decrease in I/Br-based perovskites. The first tendency is consistent with the recent experimental results.[15] For the second tendency, there are no experimental reports on the mechanical properties of Sn-based perovskites. However, we notice that it was reported from recent first-principles calculations that the bulk modulus and shear modulus of Pb-based perovskites are also larger than Sn-based perovskites in $MABX_3$ or $CsBX_3$ compounds, which is in line with our results.[12,40]

The first tendency can be explained in terms of the inorganic B–X bonds in $FABX_3$ perovskites, as listed in Table 1. We can see that the B–X bond

length in Br-based perovskites is shorter than that in I-based perovskites, which means that the B–Br bond is stronger than the B–I bond due to the smaller radius of Br compared with I. However, this bond length analysis cannot explain the second tendency. As can be seen from Tables 1–3, the Sn-based perovskites with shorter bond lengths than those in Pb-based compounds have even smaller elastic moduli. Though Sn has a smaller radius than Pb, its electronegativity[11,41] is also smaller (Fig. 3). This will induce the weaker interactions between Sn–X than Pb–X. Therefore, Sn-based perovskites show smaller elastic moduli than Pb-based materials. The bond interactions can be more accurately calculated from the pCOHP approach,[42,43] which will be discussed in more details in the following.

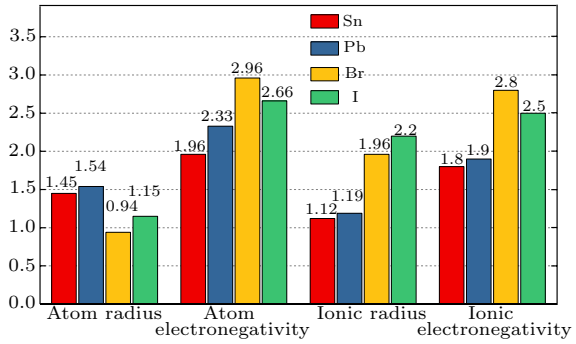

Fig. 3. The radius (Å) and electronegativity of Sn, Pb, Br and I atoms and ions.

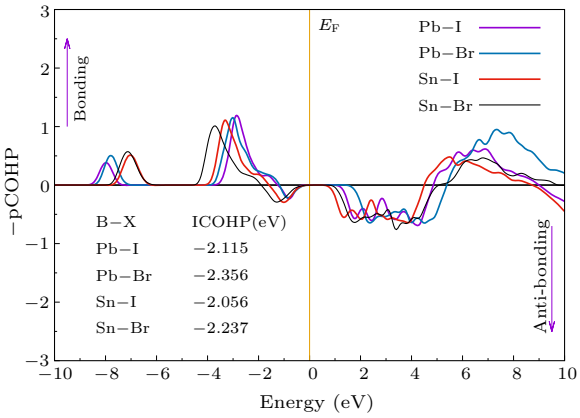

Fig. 4. COHP and ICOHP analysis of $FABX_3$.

To accurately understand the bonding characteristics of $FABX_3$ perovskites, such as B–X bonding, the newly developed pCOHP approach[42,43] is employed, which was recently introduced to investigate the hydrogen bonding in the hybrid perovskite.[39,44] Negative pCOHP values indicate bonding states, and positive pCOHP values indicate anti-bonding states. The integrated COHP (ICOHP), which reflects the bond strength (the more negative the value, the stronger the bonding strength), was also calculated.[44]

The pCOHP and ICOHP averaged over three B–X (B–X_a, B–X_b, B–X_c) atom pairs in $FABX_3$ compounds are shown in Fig. 4. The ICOHP value of Pb–Br bonding is −2.356 eV, which is stronger than the Pb–I bonding (−2.115 eV) in Pb-based perovskites, and the ICOHP value of Sn–Br (−2.237 eV) is also more negative than that of Sn–I (−2.056 eV), which provides a good explanation for the first tendency of moduli concluded above. As for replacing Pb with Sn in the compositions that have the same halogen atoms, it is found that the ICOHP value of Pb–I (−2.115 eV) is more negative than that of Sn–I (−2.056 eV) in I-based perovskites, and ICOHP value of Pb–Br (−2.356 eV) is also more negative than that of Sn–Br (−2.237 eV) in Br-based perovskites, illustrating that Pb-based perovskites exhibit a stronger B–X bond compared with Sn-based perovskites, which clearly explains the second tendency described above.

In summary, the mechanical properties of $FABX_3$ have been investigated using first-principles calculations. Our calculated results reveal that these hybrid perovskite materials are flexible and ductile, and they are suitable for compliant devices with large deformation demanded. The universal anisotropy index A^U demonstrates that these $FABX_3$ perovskites have a very strong anisotropy. It is found that the orientation of the planar organic cation FA^+ has an effect on the structure and mechanical properties of $FABX_3$ perovskites. Further, our results indicate that: (i) Replacing the I with Br, the values of bulk modulus, shear modulus and Young's modulus increase in Pb-based and Sn-based perovskites. (ii) Replacing the Pb with Sn, the values of bulk modulus, shear modulus and Young's modulus decrease in I-based and Br-based perovskites. The reasons are revealed by analyzing bonding characteristics including the atomic radius, electronegativity and pCOHP of $FABX_3$ perovskite compounds. The cases of Pb-based and Sn-based materials show that it is not enough to analyze the mechanical properties from bonding length information alone; more bonding characteristics such as electronegativity and COHP need to be taken into account. Our work may shed light on future experimental works on the mechanical properties of hybrid halide perovskites and their photovoltaic applications.

References

[1] Burschka J, Pellet N, Moon S J, Humphry-Baker R, Gao P, Nazeeruddin M K and Grätzel M 2013 *Nature* **499** 316
[2] Heo J H, Im S H, Noh J H, Mandal T N, Lim C S, Chang J A, Lee Y H, Kim H J, Sarkar A, Nazeeruddin M K, Grätzel M and Seok S I 2013 *Nat. Photon.* **7** 486
[3] https://www.nrel.gov/pv/assets/pdfs/pv-efficiency-chart.20181221.pdf
[4] Kojima A, Teshima K, Shirai Y and Miyasaka T 2009 *J. Am. Chem. Soc.* **131** 6050
[5] Yang W S, Park B W, Jung E H, Jeon N J, Kim Y C, Lee D U, Shin S S, Seo J, Kim E K, Noh J H and Seok S I 2017 *Science* **356** 1376
[6] Liu M Z, Johnston M B and Snaith H J 2013 *Nature* **501** 395
[7] Shi D, Adinolfi V, Comin R, Yuan M J, Alarousu E, Buin A, Chen Y, Hoogl, S, Rothenberger A, Katsiev K, Losovyj Y, Zhang X, Dowben P A, Mohammed O F, Sargent E H

and Bakr O M 2015 *Science* **347** 519
[8] Jiang M, Deng N H, Wang L, Xie H M and Qiu Y Q 2018 *Chin. Phys. B* **27** 67102
[9] Rolston N, Bush K A, Printz A D, Gold-Parker A, Ding Y C, Toney M F, McGehee M D and Dauskardt R H 2018 *Adv. Energy Mater.* **8** 1802139
[10] Zhao J J, Deng Y H, Wei H T, Zheng X P, Yu Z H, Shao Y C, Shield J E and Huang J S 2017 *Sci. Adv.* **3** eaao5616
[11] Feng J 2014 *APL Mater.* **2** 081801
[12] Roknuzzaman M, Ostrikov K, Wasalathilake K C, Yan C, Wang H X and Tesfamichael T 2018 *Org. Electron.* **59** 99
[13] Ferreira A C, Letoublon A, Paofai S, Raymond S, Ecolivet C, Ruffle B, Cordier S, Katan C, Saidaminov M I, Zhumekenov A A, Bakr O M, Even J and Bourges P 2018 *Phys. Rev. Lett.* **121** 085502
[14] Sun S J, Fang Y N, Kieslich G, White T J and Cheetham A K 2015 *J. Mater. Chem. A* **3** 18450
[15] Sun S J, Isikgor F H, Deng Z Y, Wei F X, Kieslich G, Bristowe P D, Ouyang J Y and Cheetham A K 2017 *ChemSusChem* **10** 3740
[16] Eperon G E, Bryant D, Troughton J, Stranks S D, Johnston M B, Watson T, Worsley D A and Snaith H J 2015 *J. Phys. Chem. Lett.* **6** 129
[17] Eperon G E, Stranks S D, Menelaou C, Johnston M B, Herz L M and Snaith H J 2014 *Energy Environ. Sci.* **7** 982
[18] Zhang Y Y, Chen S Y, Xu P, Xiang H J, Gong X G, Walsh A and Wei S H 2018 *Chin. Phys. Lett.* **35** 036104
[19] Kohn W and Sham L J 1965 *Phys. Rev.* **140** A1133
[20] Kresse G and Furthmüller J 1996 *Comput. Mater. Sci.* **6** 15
[21] Blöchl P E 1994 *Phys. Rev. B* **50** 17953
[22] Ahmad S, Kanaujia P K, Niu W, Baumberg J J and Vijaya Prakash G 2014 *ACS Appl. Mater. Interfaces* **6** 10238
[23] Lee K, Murray E D, Kong L Z, Lundqvist B I and Langreth D C 2010 *Phys. Rev. B* **82** 081101
[24] Deringer V L, Tchougréeff A and Dronskowski R 2011 *J. Phys. Chem. A* **115** 5461
[25] Maintz S, Deringer V L, Tchougréeff A L and Dronskowski R 2016 *J. Comput. Chem.* **37** 1030
[26] Yvon L P and Paul S 2002 *Phys. Rev. B* **65** 104104
[27] Weller M T, Weber O J, Frost J M and Walsh A 2015 *J. Phys. Chem. Lett.* **6** 3209
[28] Geng W, Zhang L, Zhang Y N, Lau W M and Liu L M 2014 *J. Phys. Chem. C* **118** 19565
[29] Jong U G, Yu C J, Ri G C, McMahon A P, Harrison N M, Barnes P R F and Walsh A 2018 *J. Mater. Chem. A* **6** 1067
[30] Hanusch F C, Wiesenmayer E, Mankel E, Binek A, Angloher P, Fraunhofer C, Giesbrecht N, Feckl J M, Jaegermann W, Johrendt D, Bein T and Docampo P 2014 *J. Phys. Chem. Lett.* **5** 2791
[31] Mitzi D B and Liang K 1997 *J. Solid State Chem.* **134** 376
[32] Ferrara C, Patrini M, Pisanu A, Quadrelli P, Milanese C, Tealdi C and Malavasi L 2017 *J. Mater. Chem. A* **5** 9391
[33] Wang J F, Fu X N and Wang J T 2017 *Chin. Phys. B* **26** 106301
[34] Ding Y C, Chen M, Gao X Y and Jiang M H 2012 *Chin. Phys. B* **21** 067101
[35] Wu Z J, Zhao E J, Xiang H P, Hao X F, Liu X J and Meng J 2007 *Phys. Rev. B* **76** 054115
[36] Ravindran P, Fast L, Korzhavyi P A, Johansson B, Wills J and Eriksson O 1998 *J. Appl. Phys.* **84** 4891
[37] Pugh S F 1954 *The London, Edinburgh, and Dublin Philosophical Magazine and Journal of Science* **45** 823
[38] Ranganathan S I and Ostoja-Starzewski M 2008 *Phys. Rev. Lett.* **101** 055504
[39] Tang G, Yang C, Stroppa A, Fang D N and Hong J W 2017 *J. Chem. Phys.* **146** 224702
[40] Roknuzzaman M, Ostrikov K, Wang H X, Du A J and Tesfamichael T 2017 *Sci. Rep.* **7** 14025
[41] Allred A L 1961 *J. Inorg. Nucl. Chem.* **17** 215
[42] Amat A, Mosconi E, Ronca E, Quarti C, Umari P, Nazeeruddin M K, Grätzel M and de Angelis F 2014 *Nano Lett.* **14** 3608
[43] Kato M, Fujiseki T, Miyadera T, Sugita T, Fujimoto S, Tamakoshi M, Chikamatsu M and Fujiwara H 2017 *J. Appl. Phys.* **121** 115501
[44] Shen P F, Nie K Q, Sun X H, Liu L J and McLeod J A 2016 *Physica Status Solidi (RRL)–Rapid Res. Lett.* **10** 677